A quasi solid-state dye-sensitized solar cell containing binary ionic liquid and polyaniline-loaded carbon black

Po-Yen Chen [a], Chuan-Pei Lee [a], R. Vittal [a], Kuo-Chuan Ho [a,b,*]

[a] *Department of Chemical Engineering, National Taiwan University, Taipei 10617, Taiwan*
[b] *Institute of Polymer Science and Engineering, National Taiwan University, Taipei 10617, Taiwan*

ABSTRACT

A quasi solid-state dye-sensitized solar cell (DSSC) is fabricated using 1-propyl-3-methylimidazolium iodide (PMII) and polyaniline-loaded carbon black (PACB) as the composite electrolyte. The electrolyte without added iodine is sandwiched between TiO_2 working electrode and platinum counter electrode (CE). A power conversion efficiency (η) of 5.81% is achieved with this type of cell. With the addition of 1-ethyl-3-methylimidazolium thiocyanate (EMISCN), a low-viscosity ionic liquid (IL), the cell with the binary ionic liquid (bi-IL) renders an efficiency of 6.15%, the best for any quasi solid-state DSSC without the addition of iodine. To fabricate a low cost DSSC using the bi-IL, the platinum layer of the counter electrode is replaced with a polymer layer, 3,3-diethyl-3,4-dihydro-2H-thieno-[3,4-b][1,4] dioxepine (PProdot-Et$_2$) through electrodeposition, and the corresponding DSSC shows an efficiency of 5.27%. At-rest stability of the quasi solid-state DSSC with bi-IL is compared with that of a liquid electrolyte DSSC at room temperature; the power conversion efficiency of the former shows a decrease of hardly 3% after 1000 h, while that of the latter shows a decrease of about 30%. The quasi solid-state cell shows unfailing durability at 70 °C.

© 2010 Elsevier B.V. All rights reserved.

1. Introduction

The focus of research on dye-sensitized solar cells (DSSCs) has shifted recently from those based on liquid electrolytes to quasi solid-state cells, because of the technological problems associated with the liquid electrolytes, such as hermetic sealing of the cells, evaporation of liquids at high temperatures, permeation of water and oxygen molecules into the electrolyte. Manufacturing of multi-cell modules is also a difficult task with liquid electrolyte cells for obvious reasons, especially due to the corrosive nature of iodine, one of the components of a liquid electrolyte cell. Replacing the liquid electrolyte in the DSSC with a solid or quasi solid electrolyte is expected to solve these problems. P-type inorganic semiconductors [1,2], conducting polymers [3,4], ionic liquids and gelled matrices [5–7] have been used for the solidification of liquid electrolytes. The power conversion efficiency of a quasi solid-state DSSC is presently lesser than that of a liquid electrolyte cell, because a quasi solid electrolyte cannot permeate easily into the pores of a TiO_2 film, owing to its highly viscous nature; this impermeability and viscous nature of a quasi solid electrolyte renders lesser efficiency to its DSSC.

Expensive source of the cathodic material platinum for the preparation of CEs is another factor to be considered for cost-effective fabrication of DSSCs, although platinum often shows high catalytic activity for I_3^- reduction and excellent electronic conductivity. In the case of flexible DSSC, the platinum films can only be prepared by vacuum sputtering method which is an expensive method. To overcome this issue, studies on alternative materials for CEs have been made. Several new materials, such as carbon nanotubes, activated carbon, graphite, carbon black, and conducting polymers have been investigated for CEs in DSSCs [8–11]. Polymer-based hole-transporting material has been studied for a platinum-free solid-state DSSC [12], using poly(N-vinylcarbazole) (PVK) as hole-transporter mediated by an alkali iodide formed a solid junction between two electrodes and rendered for its cell an efficiency of 2.0%.

Ikeda et al. fabricated a near solid-state DSSC, with the electrolyte containing polyaniline-loaded carbon black (PACB) and the IL, 1,3-diethyleneoxide derivative of imidazolium iodide (EOI) without the addition of iodine, and obtained an efficiency of 3.48% [13]; two other groups mentioned iodine-free DSSCs [14,15] which however showed much lesser efficiencies than the cells discussed in our study. Here lies the significance of the present work, where we have developed an iodine-free quasi solid-state DSSC which rendered a power conversion efficiency of 6.15%, the best

for any quasi solid-state DSSC without iodine. Evasion of iodine was intended to understand distinctively the function of PACB as a substitute for iodine in a quasi solid-sate DSSC and also to maintain the electrolyte to be as solid as possible; the electrolyte in our study is a near solid. Iodine-free electrolyte is desirable for flexible DSSCs where a metal substrate, such as titanium is prone to corrosion by iodine. Replacing the platinum layer with the polymer layer, 3,3-diethyl-3,4-dihydro-2H-thieno-[3,4-b][1,4] dioxepine (PProdot-Et$_2$) showed however a reduced efficiency of 5.27%. The cell in this study also shows very high stability. These types of DSSCs assume importance, because they possess high stability and are cost-effective.

2. Experimental

Poly(ethylene glycol) (PEG) (M.W. 20,000) and anhydrous 1-propyl-3-methylimidazolium iodide (PMII) were obtained from Merk; 1-ethyl-3-methylimidazolium thiocyanate (EMISCN), titanium(IV) isopropoxide (TTIP), acetonitrile (ACN), acetylacetone, ethanol, neutral cleaner, isopropyl alcohol (IPA), and 3-diethyl-3,4-dihydro-2H-thieno-[3,4-b][1,4] dioxepine (PProdot-Et$_2$) were purchased from Aldrich.

The PACB from Sigma–Aldrich Inc. contained 20 wt% polyaniline emeraldine salt (half oxidized and hydrogenated polyaniline doped with organic sulfonic acid). Conductive composite electrolyte was prepared by mixing PACB with an IL. In order to mix well, a little amount of ACN was initially added to the composite and the composite was stirred for 1 day. Then the ACN was removed slowly in vacuum to ensure complete removal. The organic solvent electrolyte containing a mixture of 0.1 M LiI, 0.6 M PMII, 0.05 M I$_2$, and 0.5 M TBP in gamma-butyrolactone (GBL, Fluka) was used.

6.0 g of commercial titanium dioxide (ST-21, 50 m^2 g^{-1}) obtained from Ya Chung Industrial Co. Ltd., Taiwan was thoroughly mixed with a solution containing 500 μl of acetylacetone and 11.0 g of DI water. This was stirred for 3 days and 1.8 g of PEG was added to the well-dispersed colloidal solution. The final mixture was stirred for an additional 2 days, and the TiO$_2$ paste was thus obtained. A fluorine-doped SnO$_2$ conducting glass (FTO, 15 Ω sq^{-1}, Solaronix S.A., Aubonne, Switzerland) was first cleaned with a neutral cleaner and then washed with DI water, acetone, and IPA, sequentially. The conducting surface of the FTO was treated with a solution of TTIP (0.028 g) in ethanol (10 ml) to obtain good mechanical contact between the conducting glass and the TiO$_2$ film, as well as to isolate the conducting glass surface from the conductive composite electrolyte. TiO$_2$ film was then coated by doctor blade method onto the treated FTO glass, which was patterned to contain TiO$_2$ portion of 0.4 cm × 0.4 cm. The TiO$_2$ film was gradually heated to 500 °C in an oxygen atmosphere, and subsequently sintered at that temperature for 30 min. After sintering and cooling to 80 °C, the TiO$_2$ film was immersed in a 3 × 10^{-4} M solution of N719 (Solaronix S.A., Aubonne, Switzerland) in acetonitrile and tert-butyl alcohol (volume ratio of 1:1) at room temperature for 24 h. For preparing CEs with conducting polymer films, PProdot-Et$_2$ was electrodeposited onto ITO glass (10 Ω sq^{-1}) by applying a constant potential of 1.1 V (vs. Ag/Ag$^+$) until the pre-determined charge capacities were reached. The slurry-like composite electrolyte was then coated onto the dye-sensitized TiO$_2$ film, while keeping the film on a hot plate at a temperature of 80 °C to ensure that the porous film was filled with the IL. The photoanode coated with composite electrolytes was then covered by the CE (platinum-sputtered or PProdot-Et$_2$-coated). The two electrodes were separated with 25 μm-thick surlyn (SX1170-60, Solaronix S.A., Aubonne, Switzerland) and held by clamps and the edges were sealed by UV glue.

The surface of the DSSC was illuminated by a class A quality solar simulator (PEC-L11, AM1.5G, Peccell Technologies, Inc.)
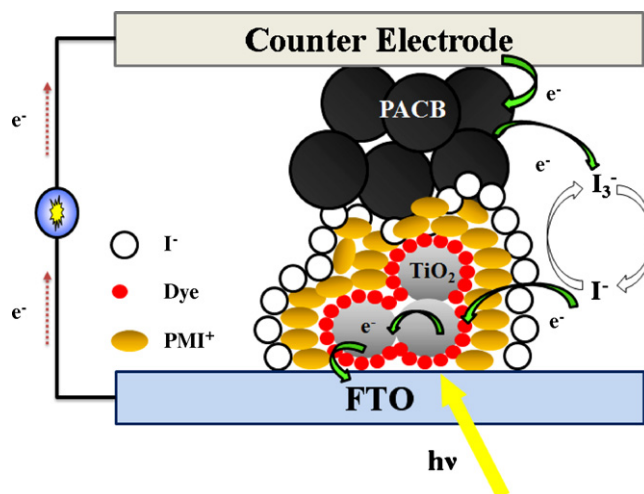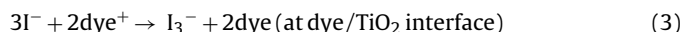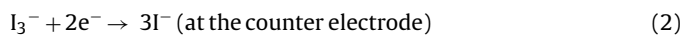

Scheme 1. Schematic representation of the operation of quasi solid-state DSSC with its composite electrolyte.

and the incident light intensity (100 mW cm^{-2}) was calibrated with a standard Si Cell (PECSI01, Peccell Technologies, Inc.). The photoelectrochemical characteristics of the DSSCs were recorded with a potentiostat/galvanostat (PGSTAT 30, Autolab, Eco-Chemie, the Netherlands). The film thickness was determined using a surface profilometer (Sloan Dektak 3030). Morphologies of the counter electrodes were observed by scanning electron microscopy (SEM, Hitachi S-4700). Electrochemical impedance spectra (EIS) were obtained by the above-mentioned potentiostat/galvanostat equipped with an FRA2 module under a constant light illumination of 100 mW cm^{-2}. The frequency range explored was 10 mHz to 65 kHz. The applied bias voltage and ac amplitude were set at the open-circuit voltage of the DSSC and 10 mV, respectively, between the FTO-TiO$_2$-dye working electrode and the CE, starting from the short-circuit condition. For electrochemical impedance analysis, an equivalent circuit model was used for interpreting the characteristics of the DSSCs [16,17].

3. Results and discussion

The quasi solid-state DSSC with a composite electrolyte consisting of PACB and an IL (such as PMII) can be represented schematically as shown in Scheme 1, where the IL functions as a carrier mediator between sensitized TiO$_2$ and PACB [13]. This cell operates in the absence of iodine, which usually is an essential component of an electrolyte in a conventional DSSC. It is well known that in a conventional DSSC iodine gives rise to triiodide ions, which in turn are required to complete the circuit by their reduction at the counter electrode to produce iodide ions, which regenerate the oxidized dye; these reactions in a conventional DSSC are as follows:

$$I^- \xleftrightarrow{I_2} I_3^- \xleftrightarrow{I_2} I_5^- \text{ (in the electrolyte)} \tag{1}$$

$$I_3^- + 2e^- \rightarrow 3I^- \text{ (at the counter electrode)} \tag{2}$$

$$3I^- + 2dye^+ \rightarrow I_3^- + 2dye \text{ (at dye/TiO}_2 \text{ interface)} \tag{3}$$

In absence of iodine in our case the source of iodide is only the IL. This does not imply that IL can replace iodine in a normal DSSC. It can be noticed in further discussions that the efficiency of a DSSC with mere IL, i.e., without additional iodine and without PACB, is only 0.18%. When we added PACB in the present research, we could get an efficiency as high as 5.81%, i.e., about 32-fold higher than that in absence of PACB. We attribute this phenomenal change in the efficiency to an extended electron transfer surface (EETS), which is

Table 1
Photovoltaic parameters of the DSSCs with composite electrolytes containing different amounts of PACB.

PACB content (wt%)	J_{SC} (mA cm^{-2})	V_{OC} (V)	η (%)	FF
16.7	12.9	0.62	3.82	0.48
11.1	12.2	0.74	5.81	0.65
9.1	10.0	0.73	5.09	0.70
6.3	9.8	0.71	4.63	0.67
0.0	0.7	0.67	0.18	0.37

formed from the counter electrode's surface and extended to the carrier mediator.

This EETS is expected to provide the catalytic effect for the reduction of I$_3$$^-$ ions [8–11]. The I$_3$$^-$ ions can be reduced to I$^-$ ions at the EETS surface (Eq. (4)) as shown in the scheme and I$^-$ can regenerate the oxidized dye, while PMII can act as carrier mediator:

$$I_3^- + 2e^- \rightarrow 3I^- \text{ (at EETS)}. \tag{4}$$

An iodide based IL provides sufficient I$^-$ for the regeneration of the oxidized dye under illumination (Eq. (3)); I$^-$ in turn oxidizes to I$_3$$^-$, which can be reduced back to I$^-$ at the EETS (Eq. (4)). Increasing content of I$_2$ increases concentration of polyiodides in the porous dye-coated TiO$_2$ matrix. It facilitates recombination of injected conduction band electrons with polyiodides, giving rise to additional dark currents. Furthermore, increasing content of I$_2$ also leads to enhanced light absorption, even in the visible range by the carrier mediator existing in the porous dye-coated TiO$_2$ matrix. This decreases the quantum of harvested light by the dye molecules [15], thereby rendering lower cell efficiency to the pertinent DSSC. Considering these aspects we avoided addition of iodine to the electrolyte in the present type of DSSC.

Table 1 summarizes photovoltaic parameters of the DSSCs with composite electrolytes containing different amounts (wt%) of PACB. It is very important to note that the efficiency is just 0.18% in the absence of PACB. The significance of PACB lies here, with which the efficiencies reached 20–30-fold higher levels than that without PACB, as can be seen in the table. The addition of PACB in the electrolyte has raised the efficiency dramatically, and a cell efficiency of 5.81% was reached with 11.1 wt% of PACB. The extraordinary increase of efficiency of the cell with PACB is attributed to the dual functions of PACB, i.e., mediating charge transfer in the electrolyte and catalyzing the I$_3$$^-$ reduction. When the amount of PACB was increased to 16.7 wt%, the cell efficiency had decreased to 3.82%; this reduced efficiency may be attributed to the increased viscosity of the composite electrolyte, which reduces its penetration into the TiO$_2$ layer and inhibits the movement of I$^-$ and I$_3$$^-$ ions.

To increase the efficiency further, we introduce the low-viscosity IL, EMISCN (25 cP at 21 °C) into PMII (900 cP at 20 °C) to form a binary ionic liquid (bi-IL). Fig. 1 shows the photocurrent–voltage characteristics of DSSCs with composite electrolytes containing 11.1 wt% PACB and the bi-IL with different volume percentages (V%) of EMISCN with respect to PMII, and Table 2 gives the corresponding values. With a volume ratio of 35/65 for EMISCN/PMII, a cell efficiency of 6.15% was achieved, indicating the beneficial effect of EMISCN. The enhancement in the

Table 2
Photovoltaic parameters and R_{ct2} values of the DSSCs with composite electrolytes containing 11.1 wt% of PACB and different volume ratios of EMISCN and PMII.

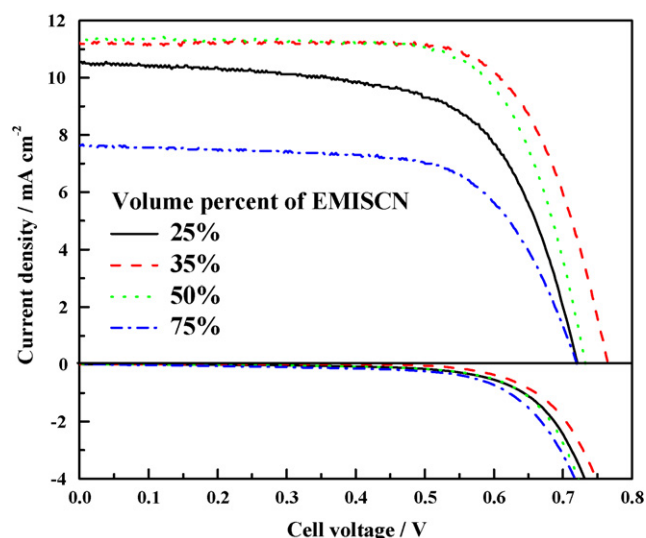| EMISCN/PMII (volume ratio)	J_{SC} (mA cm^{-2})	V_{OC} (V)	η (%)	FF	R_{ct2} (Ω)
25/75	10.6	0.72	4.87	0.64	36.6
35/65	11.2	0.76	6.15	0.72	27.3
50/50	11.4	0.74	5.94	0.71	34.9
75/25	7.6	0.72	3.64	0.60	40.5

Fig. 1. Photocurrent–voltage curves of DSSCs with composite electrolytes containing 11.1 wt% of PACB and different volume percentages of EMISCN.

efficiency of the DSSC with EMISCN, with reference to the efficiency of the best cell without this IL (5.81%) is attributed to the less viscous nature of the EMISCN, which provides better penetration of the composite electrolyte into TiO$_2$ and also better conductivity of the electrolyte for I$^-$ and I$_3$$^-$ ions. The advantages of EMISCN with regard to the improvement of the apparent diffusion coefficients and with regard to faster diffusion rates have been reported [18]. However, as the content of EMISCN exceeds 35 V%, the J_{SC}, FF and V_{OC} show a decrease in their values. The decreased J_{SC} can be related to the insufficient concentration of I$^-$ due to reduced PMII and hence inadequate dye-reduction. Two essential factors for the function of a DSSC, i.e., viscosity and concentration of I$^-$ should be complementary to each other, and this is apparently achieved at the volume ratio of 35/65 for EMISCN/PMII.

Fig. 2 shows the EIS of the DSSCs with different volume percentages of EMISCN under an illumination of 100 mW cm^{-2}, and the equivalent circuit is shown as the inset of the figure. For conventional DSSCs, the EIS spectrum usually shows three semicircles in the measured frequency range of 10 mHz to 65 kHz. The
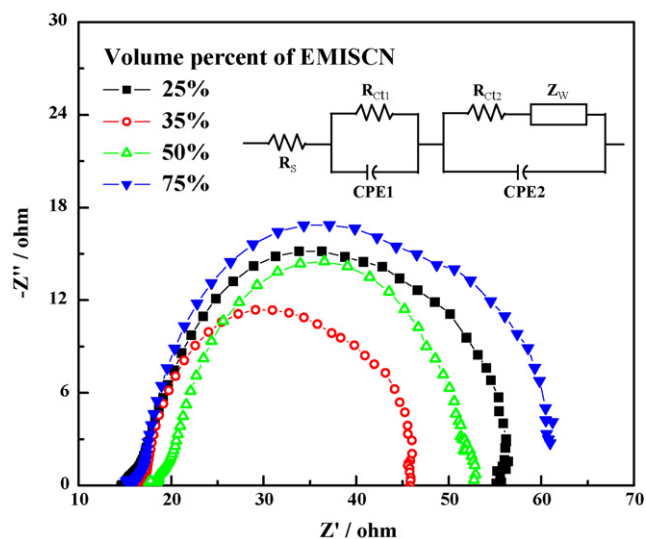

Fig. 2. EIS spectra of the DSSCs with composite electrolytes containing 11.1 wt% of PACB and different volume percentages of EMISCN with respect to PMII.

Table 3
Photovoltaics and EIS parameters of the DSSCs with different thicknesses of TiO$_2$ films.

TiO$_2$ film thickness (μm)	J_{SC} (mA cm^{-2})	V_{OC} (V)	η (%)	FF	R_{ct2} (Ω)	R_{diff} (Ω)
31.7	3.3	0.51	0.69	0.41	314.0	99.8
15.4	5.7	0.60	1.70	0.50	125.5	49.8
10.0	11.2	0.76	6.15	0.72	27.3	13.0
6.5	8.8	0.75	4.66	0.71	34.5	13.1

The composite electrolyte contains 11.1 wt% of PACB and 35 V% of EMISCN with respect to PMII.

ohmic serial resistance (R_S) corresponds to the overall series resistance. The first, second and third semi-circles correspond to the charge-transfer resistances at the counter electrode (R_{ct1}), at the TiO$_2$/dye/electrolyte interface (R_{ct2}) and to the Warburg diffusion process of I$^-$/I$_3^-$ in the electrolyte (R_{diff}), respectively. Extremely tiny R_{ct1} is observed in Fig. 2; this means, the charge transport at the CE/electrolyte interface is facile in the presence of carbon derivatives. The formation of EETS by PACB apparently facilitates electron transfer to carrier mediator as well as reduces the charge-transfer resistance at the counter electrode/electrolyte interface. Smaller R_{ct2} is observed for DSSC containing composite electrolyte with 35 V% of EMISCN in bi-IL, than those in the case of other compositions; this suggests that the balance between viscosity and concentration of I$^-$ was reached with this proportion of EMISCN in the composite electrolyte. On the other hand, an increase in R_{ct2} is noted for 50 V% of EMISCN and more in bi-IL, in consistency with our explanation for decreased J_{SC} that higher proportion of EMISCN leads to insufficient concentration of I$^-$ due to reduced PMII and hence to inadequate dye-reduction. Due to the formation of EETS, which causes shortening of diffusion length for I$^-$ and I$_3^-$, as shown
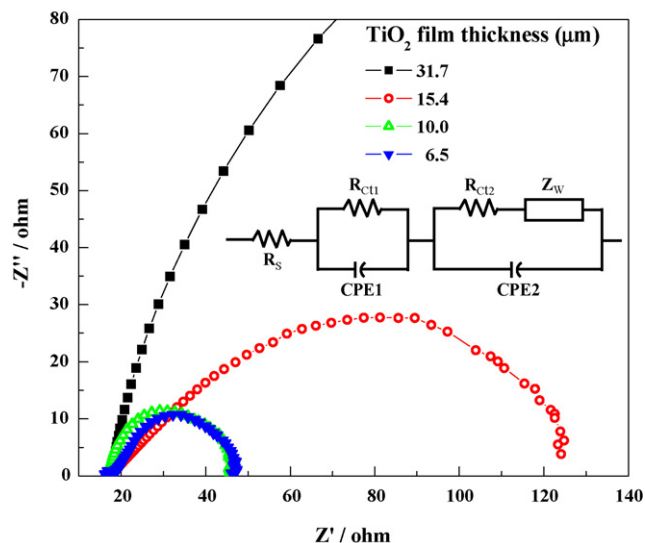

Fig. 3. EIS spectra of the DSSCs with TiO$_2$ films of different thicknesses. The composite electrolyte contained 11.1 wt% of PACB and 35 V% of EMISCN with respect to PMII.

in the scheme and represented by Eq. (4), R_{diff} is very small and is rather overlapped by R_{ct2}.

Afterward, we made an attempt to scrutinize the effect of thickness of TiO$_2$ film, using the optimum electrolyte; the photovoltaic parameters obtained for different film thicknesses under an illumination of 100 mW cm^{-2} are listed in Table 3; the table also includes the corresponding R_{ct2} and R_{diff} values. The efficiency increases
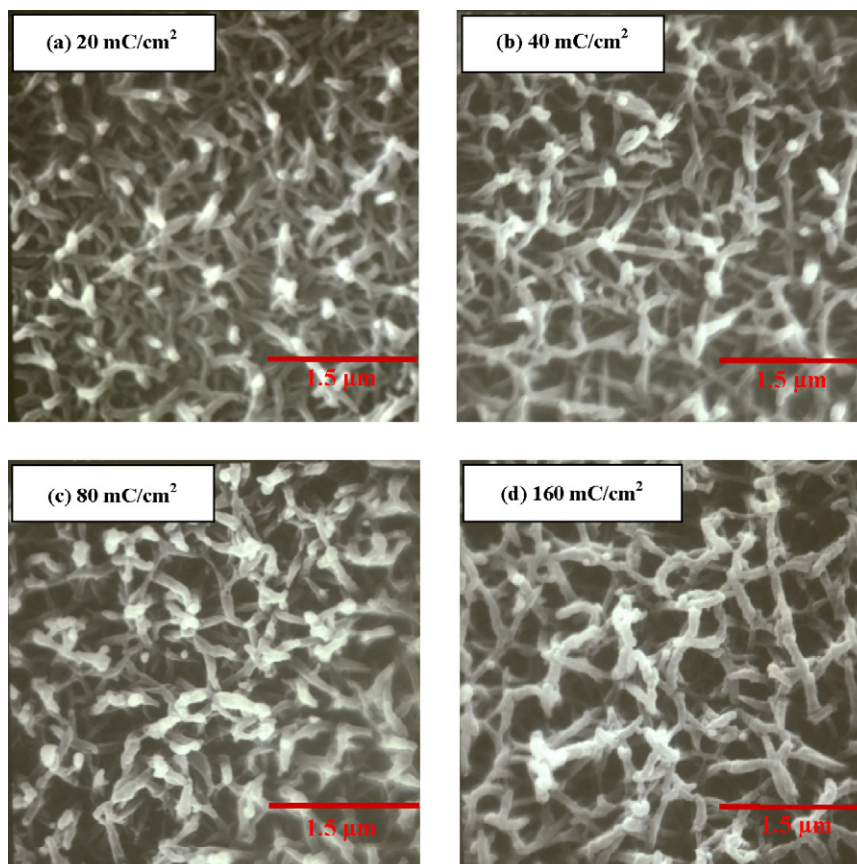

Fig. 4. SEM images of electropolymerized PProdot-Et$_2$ films obtained at different charge capacities.
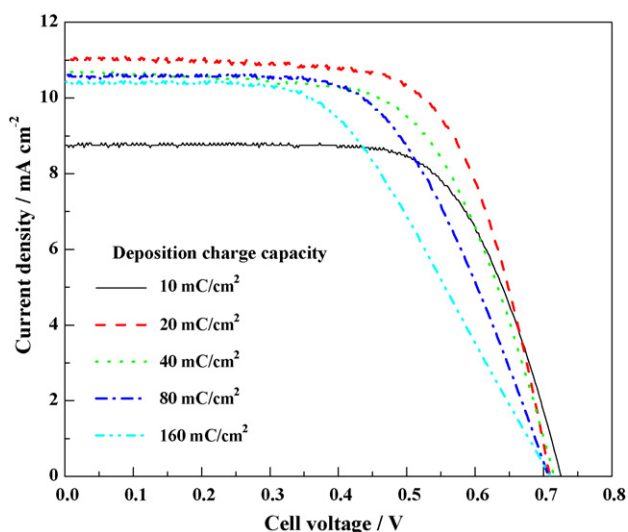
Fig. 5. Photocurrent–voltage characteristics of DSSCs with PProdot-Et$_2$-coated CEs, in which the polymer films were deposited with different charge capacities. The composite electrolyte contained 11.1 wt% of PACB and 35 V% of EMISCN with respect to PMII.

Table 4
Photovoltaic and EIS parameters of the DSSCs with PProdot-Et$_2$ CEs, where the polymer films are electrodeposited with different charge capacities.

Deposition charge capacity (mC cm^{-2})	J_{SC} (mA cm^{-2})	V_{OC} (V)	η (%)	FF	R_{ct1} (Ω)	R_{ct2} (Ω)
10	8.7	0.73	4.33	0.68	20.1	46.0
20	11.0	0.71	5.27	0.68	8.1	40.0
40	10.7	0.72	4.79	0.63	27.2	49.2
80	10.6	0.71	4.44	0.59	49.2	47.8
160	10.4	0.71	3.81	0.52	113.9	49.4

The composite electrolyte contains 11.1 wt% of PACB and 35 V% of EMISCN with respect to PMII.

capacity increases from 20 to 160 mC cm^{-2}. It is understood that the aggregation of PProdot-Et$_2$ greatly prevents the filling of its porous layer by the solid-state electrolyte, which results in an unfavorable contact and less hole-transporting positions, and thereby in a decreased FF. Further, Table 4 also shows the EIS parameters of DSSCs with PProdot-Et$_2$ layers on CEs, in which the polymer films were electrodeposited with different charge capacities. The smallest R_{ct1} was obtained at 20 mC cm^{-2} of charge capacity. Hence, we suggest that a dense porous structure of PProdot-Et$_2$ (as shown in Fig. 4a) reduces the charge transport resistance at the interface of CE and electrolyte, rather than a loose porous structure (as shown in Fig. 4d).
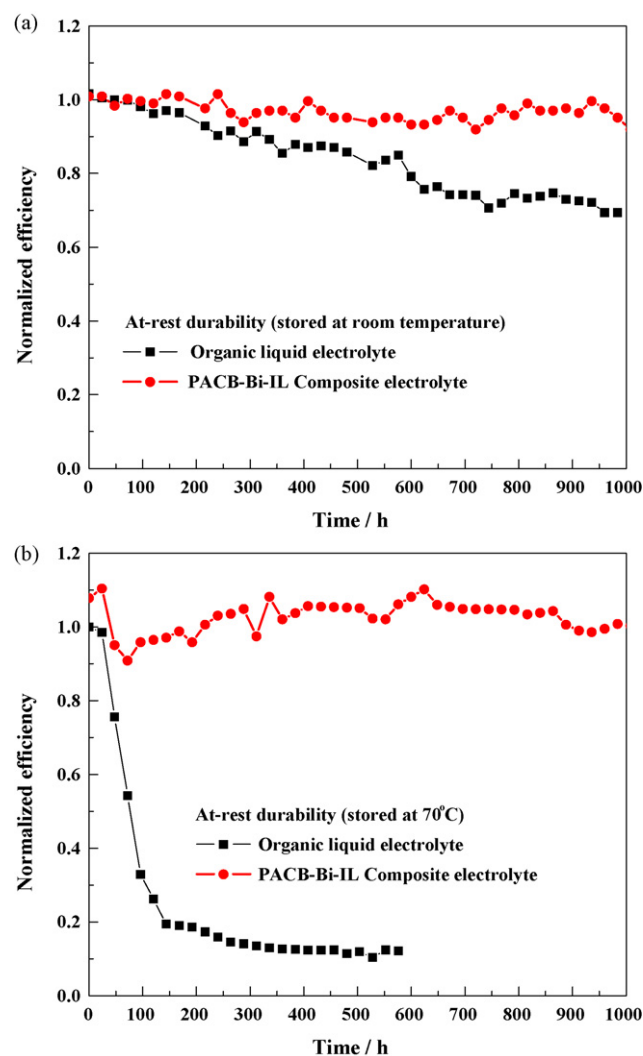

Fig. 6. At-rest durabilities of DSSCs, one with PACB-bi-IL composite electrolyte and the other with an organic liquid electrolyte.

with increasing film thickness from 6.5 to 10.0 μm and decreases for films thicker than 10.0 μm. It was reported that the declines in FF and J_{SC} result from the mass-transport limitations of carrier mediator in the porous film [19]. It is also reasonable to say that the electron transport in the TiO$_2$ film becomes increasingly difficult with an increase in its thickness, thereby causing a decrease in the J_{SC} and FF values. In the case of TiO$_2$ film thickness of 6.5 μm, the porous film available does not exceed the mass-transport limitations, however, this thickness is insufficient for dye-adsorption, and in turn reduces the J_{SC}; this reduced J_{SC} is the essential reason for the decreased efficiency of the cell with 6.5 μm TiO$_2$ film. Nyquist plots in Fig. 3 show that 10 μm TiO$_2$ film provides least interfacial resistance for carrier mediators at the TiO$_2$/dye surface.

Ikeda et al. fabricated a near solid-state DSSC with catalyst-free counter electrode, they achieved an efficiency of 3.48% for an iodine-free DSSC [13]; this is attributed to the absence of any catalyst layer on the counter electrode. We confirmed this for ourselves by using a catalyst-free counter electrode, i.e., a bare ITO electrode for a dye-sensitized solar cell. For this, composite electrolytes containing different ILs and carbon materials were used in the DSSC. We observed, in all the cases, that the device without platinum on the counter electrodes showed always a lower FF and V_{OC}, thereby a lower cell efficiency to the DSSC (results not shown); this implies, that in the case of a Pt-free DSSC, a high internal resistance exists against the electron transport at the interface of the CE and the electrolyte. In other terms, the presence of a catalyst layer is essential for the electron transfer from the counter electrode to the electrolyte.

However, in an attempt to avoid precious platinum, for the reasons mentioned already, we fabricated a quasi solid-state DSSC with a PProdot-Et$_2$-coated CE. The morphologies of PProdot-Et$_2$ films electropolymerized on ITO glasses at different charge capacities were observed by SEM, and are shown in Fig. 4. At the deposition charge capacity of 20 mC cm^{-2}, a dense and completely coated film can be seen, which shows a wire-like and tiny porous structure due to the steric effect. More aggregation and large pores appear as the deposition charge capacity reaches to 40 mC cm^{-2}. For the charge capacity of 20 mC cm^{-2}, the device showed the best performance (Fig. 5), and the corresponding V_{OC}, J_{SC}, FF and η are 0.71 V, 11.0 mA cm^{-2}, 0.68 and 5.27%, respectively (Table 4). Noticeably, the FF decreases to 0.52 gradually as the deposition charge

As expected and desired, the quasi solid-state DSSC in this study showed an excellent durability, compared with that of a cell with an organic liquid electrolyte. Fig. 6a shows at-rest durabilities of DSSCs with PACB-bi-IL composite electrolyte and organic liquid electrolyte. In this experiment, the cells are sealed by using surlyn and UV glue. The photoconversion efficiencies were measured once per day, while the cells were stored under dark at room temperature. Efficiencies were normalized to the average value of preceding 5 days. Although the overall power conversion efficiency of DSSC with organic solvent electrolyte has decreased by about 30%, the overall power conversion efficiency of the quasi solid-state device remained almost unchanged after being stored for more than 1000 h. Further, we also investigated the durability of the cell with the PACB-bi-IL composite electrolyte at 70 °C. Efficiencies were normalized to those of the first day, because according to our experience the efficiencies usually reach stable values at 70 °C within 1 day. As shown in Fig. 6b, the DSSC with the PACB-bi-IL composite electrolyte shows an extraordinary durability even at 70 °C. The cell with organic liquid electrolyte lost its efficiency virtually in no time. Thus, these results proved beyond doubt that the durability of the DSSC with PACB-bi-IL composite electrolyte is far superior to that of a cell with organic liquid electrolyte.

4. Conclusions

The quasi solid-state DSSC with a non-volatile composite electrolyte, comprising polyaniline-loaded carbon black (PACB) and the ionic liquid, PMII, without added iodine showed a power conversion efficiency of 5.81%. A higher efficiency of 6.18% was achieved with the same composite electrolyte with the addition of EMISCN (1-ethyl-3-methylimidazolium thiocyanate), the highest for any iodine-free quasi solid-state DSSC. It is concluded that PACB forms an extended electron transfer surface (EETS) to reduce the diffusion length for I^- and I_3^- ions in the electrolyte, and also simultaneously serves as a charge-transporter and a catalyst for I_3^- reduction. When we altered the counter electrode by replacing the platinum layer with a layer of PProdot-Et$_2$ (3,3-diethyl-3,4-dihydro-2H-thieno-[3,4-b][1,4] dioxepine), the cell efficiency was found to be 5.27%, when a charge capacity of 20 mC cm^{-2} was applied to deposit the polymer on the counter electrode. We also found for this type of quasi solid-state DSSC that the optimum thickness of the TiO$_2$ film is 10.0 μm. Finally, it was established that the at-rest durability of

the DSSC with the composite electrolyte at room temperature was much more superior to that of a cell with an organic solvent-based electrolyte. At 70 °C the quasi solid-state DSSC showed an unfailing stability, while the cell with liquid electrolyte lost its performance almost immediately. Thus ultimately an iodine-free, cost-effective, efficient, and durable quasi solid-state DSSC was fabricated.

References

[1] G.R.A. Kumara, M. Okuya, K. Murakami, S. Kaneko, V.V. Jayaweera, K. Tennakone, J. Photochem. Photobiol. A: Chem. 164 (2004) 183–185.
[2] B. O'Regan, D.T. Schwartz, S.M. Zakeeruddin, M. Grätzel, Adv. Mater. 12 (2000) 1263–1267.
[3] J. Zhang, Y. Yang, S. Wu, S. Xu, C. Zhou, H. Hu, B. Chen, H. Han, X. Zhao, Electrochim. Acta 53 (2008) 5415–5422.
[4] Y. Yang, C. Zhou, S. Xu, H. Hu, B. Chen, J. Zhang, S. Wu, W. Liu, X. Zhao, J. Power Sources 185 (2008) 1492–1498.
[5] J.H. Wu, S.C. Hao, Z. Lan, J.M. Lin, M.L. Huang, Y.F. Huang, Adv. Funct. Mater. 17 (2007) 2645–2652.
[6] J.P. Lee, B. Yoo, T. Suresh, M.S. Kang, R. Vital, K.J. Kim, Electrochim. Acta 54 (2009) 4365–4370.
[7] S.H. Kang, J.Y. Kim, H.S. Kim, H.D. Koh, J.S. Lee, Y.E. Sung, J. Phys. Chem. C 12 (2008) 17046–17050.
[8] K. Imoto, K. Takahashi, T. Yamaguchi, T. Komura, J. Nakamura, K. Murata, Sol. Energy Mater. Sol. Cells 79 (2003) 459–469.
[9] T.N. Murakami, S. Ito, Q. Wang, M.K. Nazeeruddin, T. Bessho, I. Cesar, P. Liska, R.H. Baker, P. Comte, P. Pechy, M. Grätzel, J. Electrochem. Soc. 153 (2006) A2255–A2261.
[10] K. Suzuki, M. Yamaguchi, M. Kumagai, S. Yanagida, Chem. Lett. 32 (2003) 28–29.
[11] Y. Saito, W. Kubo, T. Kitamura, Y. Wada, S. Yanagida, J. Photochem. Photobiol. A: Chem. 164 (2004) 153–157.
[12] N. Ikeda, T. Miyasaka, Chem. Commun. (2005) 1886–1888.
[13] N. Ikeda, K. Teshima, T. Miyasaka, Chem. Commun. (2006) 1733–1735.
[14] T. Muto, M. Ikegami, K. Kobayashi, T. Miyasaka, Chem. Lett. 36 (2007) 804–805.
[15] H. Wang, X. Liu, Z. Wang, H. Li, D. Li, Q. Meng, L. Chen, J. Phys. Chem. B 110 (2006) 5970–5974.
[16] L. Han, N. Koide, Y. Chiba, T. Mitate, Appl. Phys. Lett. 84 (2004) 2433–2435.
[17] L. Han, N. Koide, Y. Chiba, A. Islam, T. Mitate, Comptes Rendus Chimie 9 (2006) 645–651.
[18] P. Wang, S.M. Zakeeruddin, R. Humphry-Baker, M. Grätzel, Chem. Mater. 16 (2004) 2694–2696.
[19] S. Ito, S.M. Zakeeruddin, R. Humphry-Baker, P. Liska, R. Charvet, P. Comte, M.K. Nazeeruddin, P. Péchy, M. Takata, H. Miura, S. Uchida, M. Grätzel, Adv. Mater. 18 (2006) 1202–1205.